Parameter Estimation of Asymmetrical Six-Phase Induction Machines Using Modified Standard Tests

Hang Seng Che, *Member, IEEE*, Ayman Samy Abdel-Khalik, *Senior Member, IEEE*, Obrad Dordevic, *Member, IEEE*, and Emil Levi, *Fellow, IEEE*

***Abstract*—In multiphase machine drives, accuracy of the estimated machine parameters is crucial for effective performance prediction and/or control. While a great amount of work has been done on parameter estimation for three-phase machines, corresponding discussions for six-phase machine remain scarce. It has been proven in the literature that the effect of mutual leakage inductance between different winding layers has a significant impact on the equivalent machine reactance, which challenges the standard separation method of stator and rotor leakage inductances from the measured locked-rotor impedance. In this paper, parameter identification of an asymmetrical six-phase induction machine using six-phase no-load and locked-rotor tests is discussed. A zero-sequence test using an improved equivalent circuit is proposed to improve the accuracy of the estimated parameters. The concept is verified using experimental results obtained from a low-power prototype asymmetrical six-phase machine.**

***Index Terms*—Induction machines, parameter estimation, six-phase machines, zero-sequence test.**

I. Introduction

IN MODERN variable-speed electric drives, accurate knowledge of machine parameters is essential for a good control performance. Consequently, various parameter estimation methods have been proposed over the years for three-phase machines [1]–[3]. Since multiphase machines have gained popularity in the research community in the past two decades, some research efforts have been devoted to the parameter estimation for multiphase machines as well [4]–[10].

Manuscript received November 11, 2016; revised January 24, 2017; accepted February 16, 2017. Date of publication March 3, 2017; date of current version July 10, 2017.

H. S. Che is with the UM Power Energy Dedicated Advanced Centre, University of Malaya, Kuala Lumpur 59990, Malaysia (e-mail: hsche@um.edu.my).

A. S. Abdel-Khalik is with Texas A&M University at Qatar, Doha 23874, Qatar, and also with the Electrical Engineering Department, Faculty of Engineering, Alexandria University, Alexandria 21544, Egypt (e-mail: ayman.abdel-khalik@qatar.tamu.edu).

O. Dordevic and E. Levi are with the Faculty of Engineering and Technology, Liverpool John Moores University, Liverpool, L3 3AF, U.K. (e-mail: o.dordevic@ljmu.ac.uk; e.levi@ljmu.ac.uk).

Color versions of one or more of the figures in this paper are available online at http://ieeexplore.ieee.org.

Digital Object Identifier 10.1109/TIE.2017.2677349

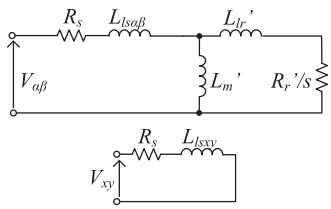

Fig. 1. Conventional VSD model (without separate mutual stator leakage inductance).

Similar to a three-phase machine, parameter estimation methods for multiphase machines are established based on specific machine equivalent circuits, particularly those governed by the vector space decomposition (VSD) model [11]. Using the VSD approach, a multiphase machine can be decomposed into several equivalent circuits that represent the decoupled vector subspaces, commonly known as the α-β (or d-q), the x-y, and the zero-sequence subspaces [12]. An example of a typical VSD-based equivalent circuit representation for a six-phase induction machine is shown in Fig. 1. Since the fundamental α-β subspace is identical to that of a three-phase machine, standard no-load and locked-rotor tests [3] (termed standard tests hereafter) seem to be readily applicable. However, this requires the knowledge of the stator to rotor leakage inductance ratio (L_{ls}/L_{lr}), which is crucial for separation of stator and rotor leakage inductance from the measured locked-rotor impedance. Unlike three-phase machines, where L_{ls}/L_{lr} has been defined in the IEEE Std-112 based on experience and empirical observations, the lack of knowledge on L_{ls}/L_{lr} hinders the direct use of standard tests in multiphase machines. Consequently, some researchers have proposed to use parameter information from the x-y [6], [7] or zero-sequence subspaces [13] together with standard tests in α-β subspace for complete parameter estimation. However, such approaches are based on the fundamental assumption that the stator leakage inductances (L_{ls}) in the x-y and zero-sequence subspaces are equivalent to the one in the α-β subspace. Though this assumption has been verified in some cases [6], [7], [13], it is not always true. As a matter of fact, it has been pointed out that the leakage inductances in the fundamental $(\alpha$-$\beta)$ and nonfundamental subspaces can be very different one from the other [8], [14], [15], depending on the machine stator

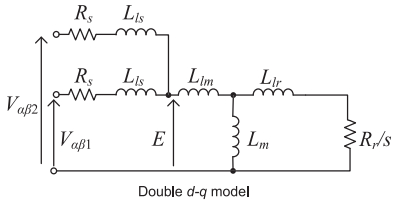

Fig. 2. Double *d*-*q* model with mutual stator leakage inductance.

winding design. Under such circumstances, aforementioned parameter estimation methods are no longer valid.

Asymmetrical six-phase machines are arguably one of the most frequently utilized multiphase machine types. Their modular three-phase structure allows the machine to be obtained from an existing three-phase machine by splitting the stator windings. Furthermore, such structure allows existing knowledge of three-phase machine to be easily extended to the six-phase machine. In terms of the machine model, the modular three-phase structure has inspired the double d-q model [16] (as shown in Fig. 2), where the equivalent circuit is essentially a modified three-phase equivalent circuit with two parallel stator branches.

Although the use of double d-q model precedes that of the VSD model, the latter has gained wider popularity and is preferred in recent works for modeling and control of six-phase machines [17], [18]. One interesting feature of the double d-q model is that it explicitly takes into account the presence of a mutual stator leakage inductance (L_{lm}), which is usually either neglected, or lumped together with L_{ls} in the VSD model. For parameter estimation, the knowledge of L_{lm} is important, as it is known to be the cause for the dissimilar leakage inductances in different subspaces [14] and can have nonnegligible impact on the steady-state performance of the machine [19].

In this paper, parameter estimation methods based on the standard tests are proposed for an asymmetrical six-phase induction machine, where the stator leakage inductances vary between different subspaces. Under such scenario, previous multiphase machine parameter estimation methods are not applicable and a new approach is required. Consequently, a new six-phase machine VSD model has been proposed, with two main modifications: the presence of L_{lm} is taken into account and the impact of rotor coupling in the zero-sequence subspace is included.

The paper is organized in the following manner. In Section II, the equivalence of the double d-q and VSD approaches is re-examined, where the presence of L_{lm} in the VSD model is explicitly expressed. Subsequently, the use of six-phase standard tests for parameter estimation is explored in Section III, where it is shown that using only no-load and locked-rotor tests is insufficient to uniquely determine all machine parameters. Then, in Section IV, special attention is devoted to the equivalent circuit in the zero-sequence subspace of the machine. By analyzing the MMF distribution, it is concluded that coupling with rotor circuit cannot be ignored in this subspace, and a new equivalent circuit is proposed to provide additional information for parameter estimation. All theoretical results are validated using experimental results shown in Section V, while concluding remarks are contained in Section VI.

II. Models of a Six-Phase Induction Machine

An asymmetrical six-phase induction machine is considered here. The machine has double-layer stator winding with winding pitch of 5/6, since this value is the most suitable value to minimize the stator leakage inductance and is used in practice in six-phase machines [14], [16]. The machine has two sets of three-phase windings, spatially displaced by an angle of 30°, with phases $a1$-$b1$-$c1$ associated with winding 1 and phases $a2$-$b2$-$c2$ associated with winding 2.

A. Double d-q Model

Unlike the VSD model, the double d-q model is obtained by applying two separate decoupling transformations, $[T_{3-1}]$ and $[T_{3-2}]$, to the variables in winding 1 and winding 2, respectively [20], [21]

$$[T_{3-1}] = \sqrt{\frac{2}{3}} \begin{matrix} \alpha 1 \\ \beta 1 \\ 0+ \end{matrix} \begin{bmatrix} 1 & -\frac{1}{2} & -\frac{1}{2} \\ 0 & \frac{\sqrt{3}}{2} & -\frac{\sqrt{3}}{2} \\ \frac{1}{\sqrt{2}} & \frac{1}{\sqrt{2}} & \frac{1}{\sqrt{2}} \end{bmatrix} \tag{1}$$

$$[T_{3-2}] = \sqrt{\frac{2}{3}} \begin{matrix} \alpha 2 \\ \beta 2 \\ 0- \end{matrix} \begin{bmatrix} \frac{\sqrt{3}}{2} & -\frac{\sqrt{3}}{2} & 0 \\ \frac{1}{2} & \frac{1}{2} & -1 \\ \frac{1}{\sqrt{2}} & \frac{1}{\sqrt{2}} & \frac{1}{\sqrt{2}} \end{bmatrix}. \tag{2}$$

The resultant $\alpha 1 - \beta 1$ and $\alpha 2 - \beta 2$ variables are used to define the machine model, as shown in Fig. 2. It is worth noting that in [20] and [21] the correlation of the parameters in the double d-q model and the VSD model has been studied. However, the derivations were again obtained based on the assumption that L_{lm} can be neglected.

B. Modified VSD Model

In [14], the effect of mutual leakage inductance on VSD model of a six-phase machine, as a function of the coil pitch, has already been investigated. However, the correlation between the obtained parameters in the VSD model and the parameters in the double d-q model, particularly L_{lm}, has not been established.

Here, the same derivation is reported for the double d-q model. This can be done by splitting the stator leakage flux (ψ_{ls}) equation in [14] and rewriting it as two sets of equations, one for each of the three-phase windings

$$\begin{aligned} [\psi_{ls1}] &= \{[L_{ls}] + [M_{lss11}]\}[i_{s1}] + [M_{lss12}][i_{s2}] \\ [\psi_{ls2}] &= \{[L_{ls}] + [M_{lss22}]\}[i_{s2}] + [M_{lss21}][i_{s1}] \end{aligned} \tag{3}$$

where

$$[i_{s1}] = [i_{a1} \quad i_{b1} \quad i_{c1}]^T \qquad [i_{s2}] = [i_{a2} \quad i_{b2} \quad i_{c2}]^T$$

$$[L_{ls}] = (L_t + L_b)[I_3]$$

$$[M_{lss11}] = [M_{lss22}] = 2M_{tb} \begin{bmatrix} k_1 & k_2 & k_2 \\ k_2 & k_1 & k_2 \\ k_2 & k_2 & k_1 \end{bmatrix}$$

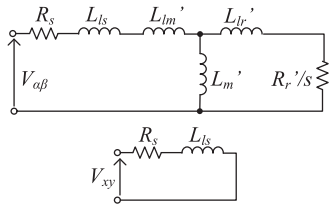

Fig. 3. α-β and *x*-*y* plane equivalent circuits for VSD model considering mutual stator leakage inductance.

$$[M_{lss12}] = [M_{lss21}]^T = 2M_{tb}\begin{bmatrix} k_3 & -k_3 & 0 \\ 0 & k_3 & -k_3 \\ -k_3 & 0 & k_3 \end{bmatrix}. \quad (4)$$

Here, L_t and L_b are the self-inductances associated with the top layer and bottom layer of the conductors in a slot, respectively; $[I_3]$ is 3×3 identity matrix; M_{tb} is the mutual inductance between the two layers and constants k_1, k_2 and k_3 are functions of the coil pitch, as given in [14].

For the double d-q model, two three-phase decoupling transformations (1) and (2) are applied onto (3), to give the following equations for the two windings:

$$\begin{bmatrix} \psi_{ls\alpha\beta1} \\ \psi_{ls\alpha\beta2} \end{bmatrix} = \left\{(L_t + L_b) + 2M_{tb}(k_1 - k_2 - \sqrt{3}k_3)\right\}\begin{bmatrix} i_{s\alpha\beta1} \\ i_{s\alpha\beta2} \end{bmatrix} + 2\sqrt{3}k_3 M_{tb}\begin{bmatrix} i_{s\alpha\beta1} + i_{s\alpha\beta2} \\ i_{s\alpha\beta1} + i_{s\alpha\beta2} \end{bmatrix}. \quad (5)$$

The equations for zero-sequence components are

$$\begin{bmatrix} \psi_{ls0+} \\ \psi_{ls0-} \end{bmatrix} = \{(L_t + L_b) + 2M_{tb}(k_1 + 2k_2)\}\begin{bmatrix} i_{s0+} \\ i_{s0-} \end{bmatrix}. \quad (6)$$

From the derivation, it can be seen that the stator leakage inductance in the α-β subspace consists of two parts:

1) a self-leakage component

$$L_{ls} = (L_t + L_b) + 2M_{tb}(k_1 - k_2 - \sqrt{3}k_3) \quad (7)$$

2) a mutual leakage component

$$L_{lm} = 2\sqrt{3}k_3 M_{tb}. \quad (8)$$

By comparing (7) and (8) with the results derived in [14], the leakage inductances for the VSD model and double d-q model can be related as follows:

$$L_{ls\alpha\beta} = L_{ls} + 2L_{lm} \qquad L_{lsxy} = L_{ls}. \quad (9)$$

Similar to the relation established in [21] and [22], apart from R_s and L_{ls}, the new VSD model can be represented by a new VSD equivalent mutual leakage inductance (L_{lm}') magnetizing inductance (L_m'), rotor leakage inductance (L_{lr}'), and rotor resistance (R_r'), whose magnitudes are twice those in the double d-q model.

$$L_{lm}' = 2L_{lm} \quad L_m' = 2L_m \quad L_{lr}' = 2L_{lr} \quad R_r' = 2R_r. \quad (10)$$

TABLE I
PARAMETERS ESTIMATED FROM SIX-PHASE TESTS

No-load test	
L_{nl}	$L_{ls} + L_{lm}' + L_m' = L_{ls} + 2(L_{lm} + L_m)$
Locked-rotor test	
R_{lock}	$R_s + R_r' = R_s + 2R_r$
L_{lock}	$L_{ls} + L_{lm}' + L_{lr}' = L_{ls} + 2(L_{lm} + L_{lr})$
x-*y* excitation test	
L_{lsxy}	L_{ls}

The new VSD equivalent circuit representation in Fig. 3 shows that the effective stator leakage inductance in the α-β subspace is larger than the one in the *x*-*y* subspace, due to the presence of the mutual leakage effect between the two stator winding sets. By measuring the impedance in the *x*-*y* subspace, L_{ls} can be directly determined. Nevertheless, even though L_{ls} is known, information from standard tests is not sufficient to identify all machine parameters, as discussed in Section III.

III. SIX-PHASE STANDARD TESTS

A. Six-Phase Standard Tests

Similar to three-phase machines, parameter estimation for asymmetrical six-phase induction machines can be done using the six-phase version of the standard no-load and locked-rotor tests. This can be performed by applying balanced asymmetrical six-phase voltages, obtained from either a transformer with dual wye-delta secondary windings [14] or a multiphase inverter [6]. Under these tests, only the α-β subspace is excited, so that the parameters obtained from the corresponding tests are given in Table I.

B. Six-Phase x-y Subspace Test

Additionally, an impedance test in the x-y subspace can be performed to identify L_{ls} (the last row in Table I). For an asymmetrical six-phase machine, this can be done by controlling appropriately a multiphase inverter [6] or by phase order transposition ($b_1 - c_1$ and $a_2 - b_2$) [12], [14]. Such voltage sequence will excite only the $x - y$ plane but not the α-β plane, so that L_{ls} can be determined from the angular frequency (ω), the measured fundamental voltage component (V_1), fundamental current component (I_1), and the phase shift between them (ϕ)

$$L_{lsxy} = L_{ls} = \frac{V_1}{\omega I_1}\sin\phi. \quad (11)$$

Although L_{ls} can be determined in this way, the described tests do not enable separation of the stator and rotor leakage inductances in the measured blocked-rotor inductance. The main problem is in the L_{lm}', which is lumped with L_m' in no-load test and with L_{lr}' in the locked-rotor test. Hence, additional information is necessary to fully estimate all machine parameters. Thus, in this paper, an additional zero-sequence test is proposed, as discussed in Section IV.

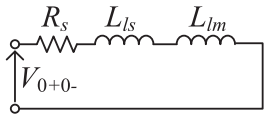

Fig. 4. Zero-sequence plane equivalent circuit for VSD model for short pitched windings $(5/6 < r < 1)$, without rotor effect.

IV. Proposed Zero-Sequence Test

A. Zero-Sequence Inductance of the Stator Windings

From [14] and (6), it is found that both double $d-q$ and VSD models have the same zero-sequence stator leakage inductance and it depends on the value of k_2

$$L_{ls0+0-} = (L_t + L_b) + 2M_{tb}(k_1 + 2k_2) = L_{ls} + L_{lm} + 6M_{tb}k_2. \quad (12)$$

For a practical winding pitch, with r that lies in the range of $5/6 < r < 1$, the value of k_2 is zero. This allows (12) to be simplified as

$$L_{ls0+0-} = L_{ls} + L_{lm}. \quad (13)$$

Consequently, the equivalent circuit for the zero-sequence subspace is given in Fig. 4. Based on Fig. 4, it appears that L_{lm} (and hence L'_{lm} which is equal to $2L_{lm}$) could be theoretically obtained from the zero-sequence inductance using standard zero-sequence test. However, this is not the case due to the nonnegligible rotor coupling effect, which is explained in Section IV-B.

B. Effect of Rotor Induced Current Under Zero-Sequence Test

In electric machines, a general assumption of zero total flux is usually made when a three-phase winding is fed with a zero-sequence current component. This assumption is true for the fundamental torque producing flux component; however, the effect of low-order harmonics will mainly depend on the winding layout. In multiphase machines, the effect of low-order harmonics cannot be ignored in all cases and should be addressed carefully.

In an asymmetrical six-phase winding, there are two zero-sequence components, with a spatial displacement of 90° between their magnetic axes. To illustrate this point, the MMF distribution for different cases, for a machine with 12-slots/pole-pair and a winding pitch of 5/6, is plotted. First, the MMF distribution is shown in Fig. 5 for the α-β current excitation. Fig. 6 shows the MMF distribution from each three-phase winding set and the resultant MMF due to both windings when all phases are connected in parallel to a single-phase supply and assumed to carry equal phase currents, i.e., $i_{s0+} = i_{s0-}$. It is clear that the magnetic axes of the flux components due to both windings are spatially displaced by 90 electrical degrees, which means that the two components are magnetically decoupled. Hence, the per-phase inductance will be theoretically the same with either one or both three-phase sets excited.

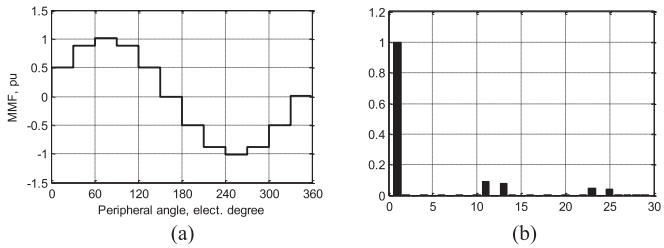

Fig. 5. MMF distribution (a) and its spectrum (b) with α-β current excitation.

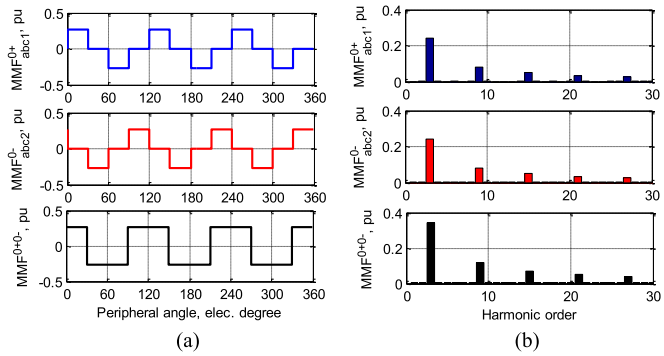

Fig. 6. MMF distributions (a) and their spectra (b) under 0+ (top row), 0- (middle row) and both zero-sequence (bottom row) current excitation.

Both three-phase winding sets exhibit a flux distribution with a number of pole-pairs equal to $3p$. The magnitude of the third-harmonic component equals 0.244 per unit (p.u.), i.e., approximately 25% of the fundamental component under α-β current excitation.

Since a cage rotor can effectively interact with all air gap flux harmonics, a nonnegligible rotor current component can be induced. It is clear that the next low-order harmonics under α-β current excitation are the 11th and 13th. Interestingly enough, the 5th and 7th are completely canceled. Nevertheless, in practical case and due to different machine asymmetries, the air gap flux may exhibit very small 5th and 7th harmonics. However, the coupling with rotor due to these small components can be merely neglected since the magnetizing coupling inductance of each of these harmonics is proportional to the square of the MMF magnitude of such a harmonic. For this reason, only the third-harmonic components need to be taken into account.

Under single-phase ac excitation, the air gap flux created by the third harmonics will have a pulsating nature. Hence, the average torque due to this flux component at zero speed will sum to zero; this is why the effect of this subspace was neglected in the literature. However, the impact of this rotor coupling should not be overlooked during parameter estimation. It is not accurate to assume that the zero-sequence impedance can be simply represented by the stator resistance and the sum of the stator self- and mutual leakage inductances $L_{ls0+0-} = L_{ls} + L_{lm}$. The effect of the rotor circuit should be included. Due to this, it is also expected that the zero-sequence resistance will be higher than the stator resistance.

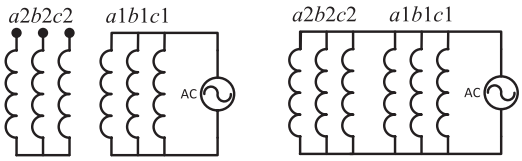

Fig. 7. Connections for zero-sequence test using three-phase excitation (left) and six-phase excitation (right).

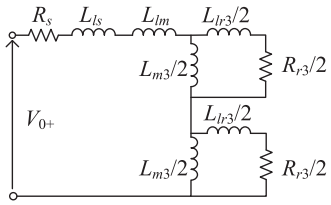

Fig. 8. Improved zero-sequence equivalent circuit.

It is worth noting that zero-sequence test for a six-phase machine can be conducted using either three-phase excitation or six-phase excitation. The former is done by applying a single-phase ac source across all three phases of one three-phase winding connected in parallel, while the latter excites all six phases in parallel, as illustrated in Fig. 7. Both approaches result in a pulsating air gap flux, but with some slight differences between them. Since magnetic axes of the two components are in quadrature (i.e., they are spatially displaced by 90° in electrical angle), the magnitude of the fundamental of the resultant MMF distribution under a six-phase excitation (which is the third harmonic) will be $\sqrt{2}$ times the magnitude of the corresponding MMF component produced by separate three-phase windings, as illustrated in Fig. 6.

Furthermore, the difference between the equivalent resistance and stator resistance under six-phase excitation will be twice the same difference under three-phase excitation, since the magnitude of the third-harmonic flux component is increased by a factor of $\sqrt{2}$, which yields the same gain in the induced rotor voltage and current. Hence, the rotor copper losses increase by a factor of $(\sqrt{2})^2 = 2$. This doubles the equivalent rotor resistance when reducing rotor circuit to the stator side. This will be confirmed in experimental results later.

Since the air gap flux in this case has a pulsating nature, the most appropriate equivalent circuit that can be used as a representation will be similar to the equivalent circuit of a single-phase induction machine in locked-rotor condition. As it has been mentioned before, since the magnetic axes of the both windings under zero-sequence excitation are in quadrature, both circuits are decoupled. Hence, three-phase excitation will be enough to carry out this test.

The proposed equivalent circuit for three-phase zero-sequence test is shown in Fig. 8. The magnetizing inductance for the third harmonic (L_{m3}) can be represented in terms of the fundamental magnetizing inductance $L_{m1}\,(=L_m)$ using a scaling factor K_{m31}

$$L_{m3} = K_{m31} L_{m1}. \tag{14}$$

The per-phase input impedance is then

$$R_{\text{zero}} + jX_{\text{zero}} = R_s + j\omega\left(L_{ls} + L_{lm}\right) + \frac{j\omega K_{m31} L_{m1}\left(R_{r3} + j\omega L_{lr3}\right)}{R_{r3} + j\omega\left(L_{lr3} + K_{m31} L_{m1}\right)}. \tag{15}$$

This complex equation leads to two real equations

$$R_{\text{zero}} = R_s + \frac{R_{r3}(\omega K_{m31} L_{m1})^2}{(R_{r3})^2 + \omega^2 (L_{lr3} + K_{m31} L_{m1})^2} \tag{16}$$

$$X_{\text{zero}} = \omega\left(L_{ls} + L_{lm} + \frac{K_{m31} L_{m1}\left({R_{r3}}^2 + \omega^2 L_{lr3}\left(L_{lr3} + K_{m31} L_{m1}\right)\right)}{(R_{r3})^2 + \omega^2 (L_{lr3} + K_{m31} L_{m1})^2}\right) \tag{17}$$

which can be solved together with the equations obtained from the no-load and locked-rotor tests.

The equivalent rotor resistance and inductance of the zero-sequence subspace can be found as functions of those of the fundamental subspace as follows. The rotor resistance and leakage inductance referred to the stator side can be found as functions of the equivalent bar and end ring segment resistance (r_{be}) and inductance (l_{be}) as [8]

$$R_{rk} = \frac{4m}{S_r}\left(\frac{T_{ph} K_{w(k)}}{K_{\text{skew}(k)}}\right)^2 r_{be} \tag{18}$$

$$L_{lrk} = \frac{4m}{S_r}\left(\frac{T_{ph} K_{w(k)}}{K_{\text{skew}(k)}}\right)^2 l_{be} \tag{19}$$

where m is the number of stator phases, T_{ph} is the number of turns per phase, $K_{w(k)}$ is the stator winding factor for any harmonic order k, S_r is the number of rotor bars, and $K_{\text{skew}(k)}$ is the cage rotor skewing factor for any harmonic order k and is given by

$$K_{\text{skew}(k)} = \sin\left(\frac{k\delta}{2}\right) \Big/ \left(\frac{k\delta}{2}\right) \tag{20}$$

where δ is the rotor skew angle. In practice, skew angle of one stator slot is usually used.

Hence, the rotor parameters of the zero-sequence subspace can be put in the following form:

$$\begin{aligned} R_{r3} &= C_{31} R_{r1} \\ L_{lr3} &= C_{31} L_{lr1} \end{aligned} \tag{21}$$

where

$$C_{31} = \left(\frac{K_{\text{skew}1}}{K_{w1}} \times \frac{K_{w3}}{K_{\text{skew}3}}\right)^2. \tag{22}$$

According to the winding function theory, the relation between the magnetizing inductance of the fundamental subspace and the zero-sequence subspace should follow the rule [8]

$$K_{m31} = \frac{L_{m3}}{L_{m1}} = \left(\frac{K_{w3}}{k K_{w1}}\right)^2. \tag{23}$$

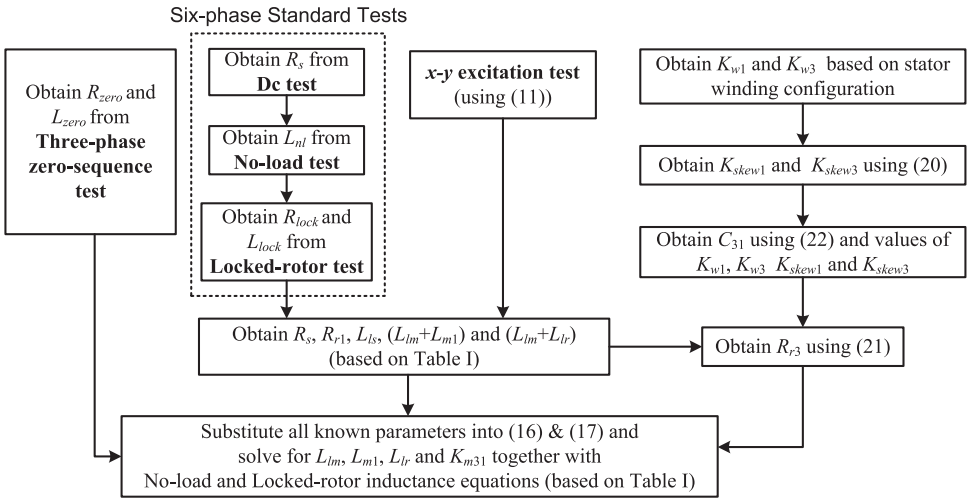

Fig. 9. Flowchart showing the complete parameter estimation procedure.

By solving these equations, machine parameters L_{ls}, L_{lm}, L_{m1}, L_{lr1} and K_{m31} can be obtained. Other parameters (e.g., L_{m3}, L_{lr3}) are normally of no importance as they relate only to the zero-sequence components and the machine is usually operated with two isolated neutral points.

The overall parameter estimation method based on aforementioned tests is illustrated in Fig. 9. The "fsolve" function in MATLAB has been used to solve the final four nonlinear equations to obtain the estimated parameters (bottom block in Fig. 9). Note that K_{m31} is assumed unknown in this identification technique. The value obtained from (23) is used as an initial guess when solving the obtained nonlinear equations using numerical solvers. The factor that needs to be calculated, which depends on machine geometric data, is C_{31}.

V. Experimental Results

To verify the presented theoretical discussion, the above-described tests are applied to a small asymmetrical six-phase induction machine, obtained by rewinding a six-pole 50 Hz, 380 V (220 V phase-to-neutral), 930 r/min three-phase induction machine. The six-phase machine is configured with double layer winding with short winding pitch of 5/6, with the same copper volume. The new rated phase voltage of the six-phase machine is 110 V with the same 1.75 A rated current. As a result of the double-layer winding and the winding pitch, the effect of the mutual stator leakage inductance should be carefully investigated. The stator resistance is first determined using dc test, and is found to be 12.5 Ω. For the standard tests, which are essentially ac tests, the stator resistance will be approximately 1.1 times larger, i.e., 13.75 Ω. This value will be used for relevant calculations in the parameter estimation test.

A. Six-Phase Standard Tests

For the six-phase standard tests, a custom made voltage source converter is used to supply the machine with the six-phase voltage. The voltage is applied at a constant frequency of 50 Hz, using open-loop controller in the α-β plane. Dual PI controllers

TABLE II
Parameters Determined From the Six-Phase Standard Tests

L_{nl}	639 mH
R_{lock}	25.3 Ω
L_{lock}	71.5 mH
L_{lsxy}	5.3 mH

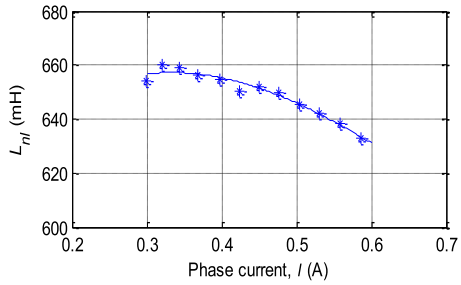

Fig. 10. No-load inductance obtained from the six-phase test.

(one PI in the synchronous reference frame, another in the antisynchronous reference frame) are used to provide closed-loop current control in the $x-y$ plane, keeping the $x-y$ current at zero at all times. This helps to reduce the unwanted effects due to the machine/converter inherent asymmetry. Phase currents and voltages are measured using oscilloscope and fast Fourier transform is performed using MATLAB to extract the fundamental components and phase angles. Measurements are done on all six phases and the results are averaged, giving values in Table II. Figs. 10–12 show the no-load inductance, the locked-rotor inductance, and the locked-rotor resistance obtained from the six-phase standard tests.

Next, the connections between the converter and the machine are rearranged (according to the discussion in Section III-B), so that the $x-y$ plane is excited instead. From this test, equivalent inductance of the $x-y$ plane, L_{xy} can be determined, as shown in Fig. 13. This is equivalent to the stator leakage inductance

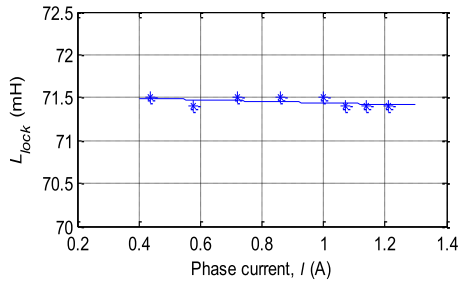

Fig. 11. Locked-rotor inductance obtained from the six-phase test.

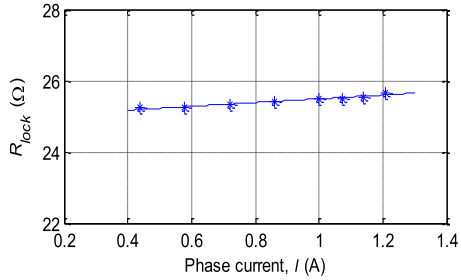

Fig. 12. Locked-rotor resistance obtained from the six-phase test.

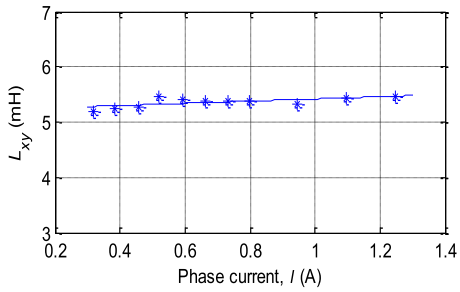

Fig. 13. Inductance obtained from the *x-y* plane excitation.

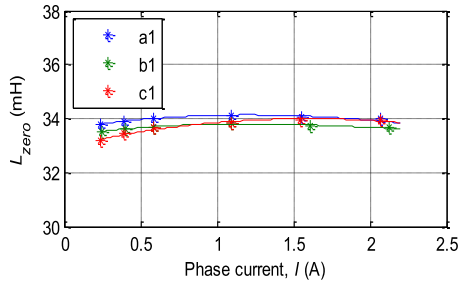

Fig. 14. Zero-sequence inductance obtained from the three-phase zero-sequence test.

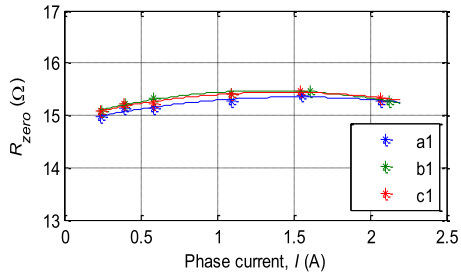

Fig. 15. Zero-sequence resistance obtained from the three-phase zero-sequence test.

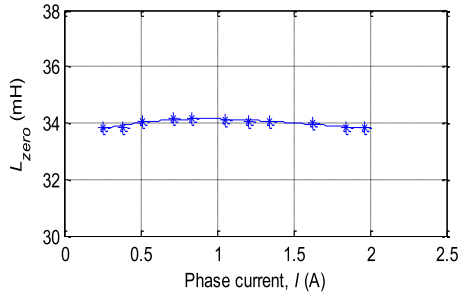

Fig. 16. Zero-sequence inductance obtained from the six-phase zero-sequence test.

L_{ls}, according to (9). The experimental results show that L_{ls} is exceptionally small compared to the locked-rotor inductance, which is $L_{\text{lock}} = L_{ls} + 2(L_{lm} + L_{lr})$. Based on this relation, the sum of mutual leakage and rotor leakage inductance is approximately 33.1 mH. Additional zero-sequence test is hence necessary to separate L_{lm} from L_{lr}, in the hope of obtaining a more accurate estimate of the machine's parameters.

B. Zero-Sequence Test

As the final test to identify the machine's parameters, zero-sequence tests are conducted. As mentioned in Section IV-B, zero-sequence test can be done with either three-phase or six-phase excitation.

The zero-sequence inductance and resistance for the three-phase zero-sequence tests are plotted in Figs. 14 and 15, respectively. These are the inductance and resistance obtained when 50 Hz single-phase ac voltage supply is applied across three parallel-connected phase windings in one three-phase winding set. As expected, the zero-sequence resistance is higher than R_s due to the coupling effect of the rotor, as seen in Fig. 8.

In order to confirm the theoretical analysis in Section IV-B, six-phase zero-sequence test is also done, and the zero- sequence inductance and resistance are given in Figs. 16 and 17, respectively. Comparison of Figs. 15 and 17 shows that the difference between equivalent resistance and stator resistance [governed by (16)] under six-phase excitation is approximately twice the difference under three-phase excitation. This confirms correctness of the theoretical derivation in Section IV.

The testing and the described procedure enable full separation of identified machine parameters, as discussed in Section V-C.

C. Estimated Machine Parameters

Generally, the effect of different operating conditions has been already discussed in the literature for multiphase induction machine [6], [8]. Even though the equivalent circuits used

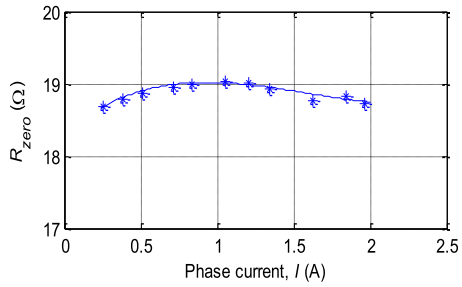

Fig. 17. Zero-sequence resistance obtained from the six-phase zero-sequence test.

TABLE III
ESTIMATED PARAMETERS FOR THE PROTOTYPE MACHINE

R_s	13.75 Ω	$R_r = R_{r1}$	5.775 Ω	R_{r3}	4.32 Ω
L_{ls}	5.3 mH	L_{lm}	20.4 mH	$L_{lr} = L_{lr1}$	12.7 mH
L_{lr3}	8.26 mH	$L_m = L_{m1}$	296.5 mH	L_{m3}	17.8 mH

for the parameter estimation tests proposed here are slightly different, their main function is to allow segregation of the leakage inductances (L_{ls}, L_{lm}, and L_{lr}), enabling a more accurate parameter estimation and hence a better performance prediction. The findings regarding the effects of operating conditions on estimated parameters, given in [6], [8], are still valid and this is therefore not addressed here. Instead, only the parameter values at rated conditions are estimated.

The results of the developed parameter estimation technique are given in Table III; the values correspond to the double $d-q$ equivalent circuit of Fig. 2. Corresponding parameters for the developed VSD model can be obtained using Table III and correlations in (10). It is worth noting that in normal operation with isolated neutrals, the zero-sequence subspace has no effect on the machine performance. However, the main benefit of estimating the parameters of this subspace is to obtain an improved estimate for L_{lm}. Other parameters of the zero-sequence subspace can be then discarded.

D. Machine Characteristic Curves

To verify the accuracy of the estimated parameters, the experimentally obtained and simulated characteristic curves of the prototype machine are compared. In order to determine the machine characteristic curves, the machine is coupled to a dc machine to act as a mechanical load. A description of the equipment and the procedure used to obtain the machine characteristics experimentally is provided in the Appendix.

The theoretical characteristic curves depend only on the parameters of the α-β plane and are calculated based on the equivalent circuit given in Fig. 1, in three different ways. In all three cases iron core loss is included, by adding the equivalent iron loss resistance, obtained from the no-load test, in the circuit of Fig. 1. It is connected in parallel to the magnetizing inductance, its value is 2700 Ω, and its existence has been neglected in the parameter estimation process. Stray load losses and mechanical losses are neglected in the calculations (although the latter was identified in a separate test for the two coupled machines). In Method 1, the locked-rotor leakage inductance is simply split into equal stator and rotor leakage inductance ($L_{ls\alpha\beta} = L_{ls}\,(=2L_{lr}) = L_{\text{lock}}/2 = 35.7\,\text{mH}$). In Method 2, the stator leakage inductance is taken as given by the $x-y$ plane test ($L_{ls\alpha\beta} = L_{lsxy} = L_{ls} = 5.3\,\text{mH}$), while the difference between the locked-rotor inductance and $x-y$ inductance is attributed to the rotor leakage inductance ($2L_{lr} = 66.2\,\text{mH}$). Finally, in Method 3 the values given in Table III are used, so that $L_{ls\alpha\beta} = L_{ls} + 2L_{lm} = 46.1\,\text{mH}$ and $2L_{lr} = 25.4\,\text{mH}$.

The comparison of theoretical curves, obtained using these three different calculation methods, with experimentally obtained results is shown in Fig. 18. It is obvious that the Method 2, which accurately takes stator leakage inductance from the x-y plane test, gives the worst fit with the experimental values, since the stator mutual leakage inductance gets incorrectly lumped

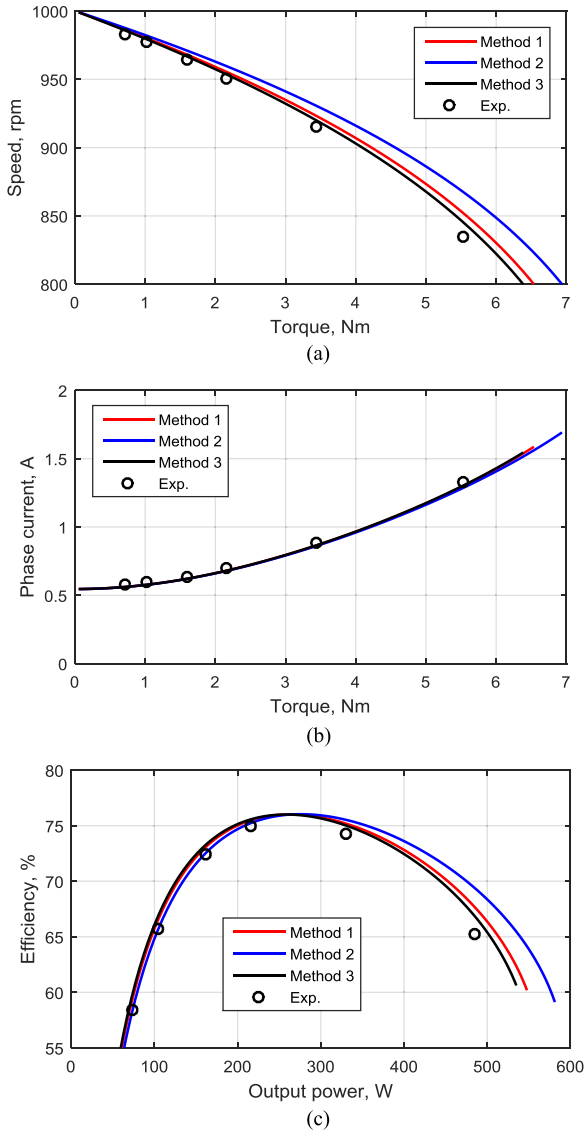

Fig. 18. Comparison between estimated and experimental characteristic curves: (a) speed/torque curve, (b) current/torque curve, and (c) efficiency/output power curve.

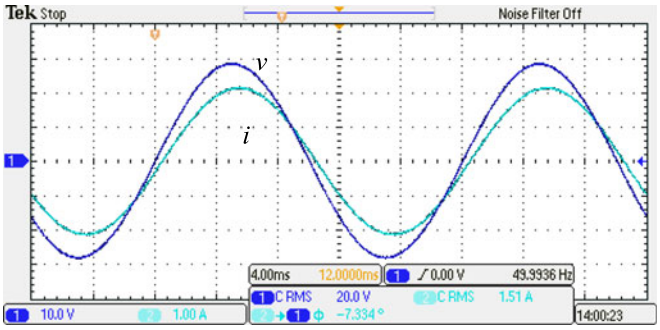

Fig. 19. Applied phase voltage and measured phase current for the machine supplied with the winding connected to the source using phase transposition.

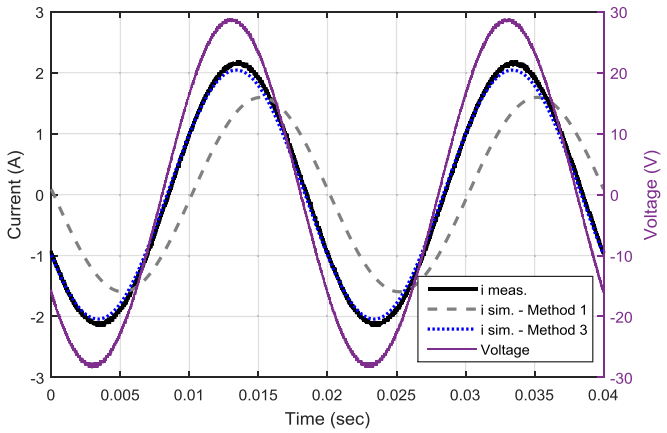

Fig. 20. Comparison of the experimentally recorded current of Fig. 19, with *x-y* plane excited, with predictions given by Method 1 and Method 3.

with the rotor leakage inductance. On the other hand, Method 1 in which locked-rotor inductance is simply split equally into stator and rotor leakage inductance provides reasonably accurate result for the characteristics in the α-β plane. As can be seen from Fig. 18, the proposed parameter identification technique gives a very good agreement between the measured and theoretical values.

Using a wrong value of the stator leakage inductance in the x-y plane would lead to a large error in prediction of the stator current harmonics in that plane. Since accurate separation of the mutual stator leakage inductance from stator and rotor leakage inductances is enabled with Method 3, the prediction of the machine behavior in the x-y plane will also be very accurate, as shown in Section V-E.

The three methods lead to a different value of the rotor time constant, which is required for indirect rotor flux oriented control and which governs the dynamics of the drive and response accuracy. Rotor leakage inductance, obtained using Method 1 to Method 3, is 17.85, 33.1, and 12.7 mH, respectively. However, as the magnetizing inductance is 296.5 mH, the ratio of the maximum (Method 2) to minimum (Method 3) rotor time constant is only 1.066. Such a small variation of the rotor time constant causes minute differences in the dynamic response that cannot be detected experimentally [1].

E. Behavior in the x-y Plane

To illustrate the importance of correct stator leakage inductance identification in the second plane, the following experiment is performed. A six-phase system of sinusoidal voltages is created as described in the Appendix, and it is then applied to the machine at standstill. To excite only the *x-y* plane, the same principle of phase transposition as in Section III-B is used when connecting source six-phase voltages to the machine phases. The six-phase voltages are selected with 50 Hz, 20-V rms values. Fig. 19 shows experimentally recorded phase voltage and current of one phase.

Next, the phase current is calculated using the two different values of the stator leakage inductance that correspond to Method 1 and Method 3 (35.7 and 5.3 mH; value in Method 2 is the same as for Method 3 in the *x-y* plane). The results are compared in Fig. 20 against the measured current of Fig. 19. It is evident that the stator leakage inductance of 5.3 mH provides far superior agreement with the measurements than the value in Method 1. The same impact would have been experienced in a voltage source inverter fed machine in relation to the current ripple prediction. This analysis confirms the correctness of the identified stator self-leakage inductance in (7).

F. Summary

On the basis of the results reported in the previous two sections, the following can be concluded.

1) Method 1 (splitting of the locked-rotor test inductance equally into stator and rotor leakage inductance) enables reasonably good prediction of the performance in the first plane but gives a poor prediction of the behavior in the second plane.
2) Method 2 (taking total stator leakage inductance in the first plane as equal to the one in the second plane and lumping the mutual stator leakage inductance with the rotor leakage inductance) gives correct prediction of the behavior in the second plane, but a very poor performance prediction in the first plane.
3) Method 3, developed here, with accurate separation of all the leakage inductance components, enables accurate prediction of the performance in both planes.

VI. Conclusion

In this paper, an improved parameter estimation technique for asymmetrical six-phase induction machines has been proposed. Two main modifications to the machine model have been suggested, resulting from consideration of the effect of the mutual stator leakage inductance and the influence of rotor induced currents in the zero-sequence subspace. It was shown that the proposed model allows all machine parameters to be estimated using six-phase standard tests together with *x-y* excitation test and a zero-sequence impedance test. Experimental results showed a very good match of machine characteristic curves and current in the x-y plane with simulated ones, confirming the validity of the presented parameter estimation method.

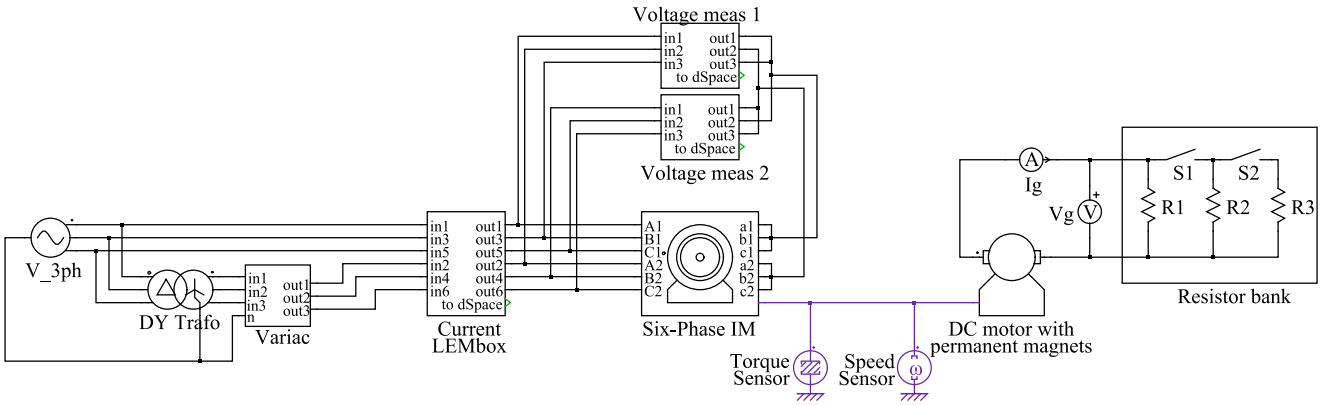

Fig. 21. Schematic of the experimental setup used to obtain experimental values in Fig. 18.

Appendix

Schematic representation of the applied measurement procedure is shown in Fig. 21. A linear four-quadrant Spitzenberger & Spies amplifier was used to generate three-phase voltage input 110-V rms, 50 Hz for the first winding. The required supply for the second winding was created using delta-wye transformer. Equal 110-V rms voltage in both three-phase systems was achieved by means of an autotransformer. Voltages were monitored using an oscilloscope. Currents and voltages were measured in all the six phases using Honeywell CSNE151-100 current sensors and LEM LV25-P voltage transducers, respectively. Measured current and voltage values were passed, using dSpace ADC board ds2004, for further processing into the dSpace 1006 system. To calculate the input active power, moving average filter principle was used and input power was calculated for each phase separately. In a similar way, voltage and current rms values were also calculated. Five periods of signal were saved (time duration 0.1 s). The sampling rate of dSpace was 20 kHz.

Output power was obtained from measured speed and torque values. Torque/speed Magtrol Torquemaster TM210 sensor was used for this purpose.

References

[1] H. A. Toliyat, E. Levi, and M. Raina, "A review of RFO induction motor parameter estimation techniques," *IEEE Trans. Energy Convers.*, vol. 18, no. 2, pp. 271–283, Jun. 2003.

[2] Y. He, Y. Wang, Y. Feng, and Z. Wang, "Parameter identification of an induction machine at standstill using the vector constructing method," *IEEE Trans. Power Electron.*, vol. 27, no. 2, pp. 905–915, Feb. 2012.

[3] *Standard Test Procedure for Polyphase Induction Motors and Generators*, IEEE Std 112 -2004, 2004.

[4] A. Gautam, O. Ojo, M. Ramezani, O. D. Momoh, and F. Wayne, "Computation of equivalent circuit parameters of nine-phase induction motor in different operating modes," in *Proc. IEEE Energy Convers. Congr. Expo.*, 2012, pp. 142–149.

[5] J. A. Riveros, F. Barrero, M. J. Duran, B. Bogado, and S. Toral, "Estimation of the electrical parameters of a five–phase induction machine using standstill techniques. Part I: Theoretical discussions," in *Proc. 37th Annu. Conf. IEEE Ind. Electron. Soc.*, 2011, pp. 3668–3673.

[6] A. G. Yepes, J. A. Riveros, F. Barrero, L. Oscar, M. Jones, and E. Levi, "Parameter identification of multiphase induction machines with distributed windings—Part 1: Sinusoidal excitation methods," *IEEE Trans. Energy Convers.*, vol. 27, no. 4, pp. 1056–1066, Dec. 2012.

[7] J. A. Riveros *et al.*, "Parameter identification of multiphase induction machines with distributed windings—Part 2: Time-domain techniques," *IEEE Trans. Energy Convers.*, vol. 27, no. 4, pp. 1067–1077, Dec. 2012.

[8] A. S. Abdel-Khalik, M. I. Daoud, S. Ahmed, A. A. Elserougi, and A. M. Massoud, "Parameter identification of five-phase induction machines with single layer windings," *IEEE Trans. Ind. Electron.*, vol. 61, no. 10, pp. 5139–5154, Oct. 2014.

[9] S. Kallio, J. Karttunen, P. Peltoniemi, P. Silventoinen, and O. Pyrhönen, "Online estimation of double-star IPM machine parameters using RLS algorithm," *IEEE Trans. Ind. Eelctron.*, vol. 61, no. 9, pp. 4519–4530, Sep. 2014.

[10] S. Kallio, J. Karttunen, P. Peltoniemi, P. Silventoinen, and O. Pyrhönen, "Determination of the inductance parameters for the decoupled d–q model of double-star permanent-magnet synchronous machines," *IET Elect. Power Appl.*, vol. 8, no. 2, pp. 39–49, 2014.

[11] Y. Zhao and T. A. Lipo, "Space vector PWM control of dual three-phase induction machine using vector space decomposition," *IEEE Trans. Ind. Appl.*, vol. 31, no. 5, pp. 1100–1109, Sep./Oct. 1995.

[12] E. Levi, "Multiphase electric machines for variable-speed applications," *IEEE Trans. Ind. Electron.*, vol. 55, no. 5, pp. 1893–1909, May 2008.

[13] C. B. Jacobina, C. C. De Azevedo, C. R. Da Silva, A. M. N. Lima, and E. R. C. Da Silva, "On-line estimation of the stator resistance of a six-phase induction machine," in *Proc. IEEE Ind. Appl. Soc. Conf.*, 2002, pp. 746–751.

[14] D. Hadiouche, H. Razik, and A. Rezzoug, "On the modeling and design of dual-stator windings to minimize circulating harmonic currents for VSI fed AC machines," *IEEE Trans. Ind. Appl.*, vol. 40, no. 2, pp. 506–515, Mar./Apr. 2004.

[15] M. Mengoni *et al.*, "Online detection of high-resistance connections in multiphase induction machines," *IEEE Trans. Power Electron.*, vol. 30, no. 8, pp. 4505–4513, Aug. 2015.

[16] T. A. Lipo, "A d-q model for six phase induction machines," in *Proc. Int. Conf. Elect. Mach.*, 1980, pp. 860–867.

[17] H. S. Che, E. Levi, M. Jones, W. P. Hew, and N. A. Rahim, "Current control methods for an asymmetrical six-phase induction motor drive," *IEEE Trans. Power Electron.*, vol. 29, no. 1, pp. 407–417, Jan. 2014.

[18] C. Zhou, G. Yang, and J. Su, "PWM strategy with minimum harmonic distortion for dual three-phase permanent-magnet synchronous motor drives operating in the overmodulation region," *IEEE Trans. Power Electron.*, vol. 31, no. 2, pp. 1367–1380, Feb. 2016.

[19] N. Amiri, S. Ebrahimi, M. Chapariha, J. Jatskevich, and H. W. Dommel, "Voltage-behind-reactance model of six-phase synchronous machines considering stator mutual leakage inductance and main flux saturation," *Elect. Power Syst. Res.*, vol. 138, pp. 155–164, 2016.

[20] R. Bojoi, M. Lazzari, F. Profumo, and A. Tenconi, "Digital field-oriented control for dual three-phase induction motor drives," *IEEE Trans. Ind. Appl.*, vol. 39, no. 3, pp. 752–760, May–Jun. 2003.

[21] R. Bojoi, "Analysis, design and implementation of a dual three-phase vector controlled induction motor drive," Ph.D. dissertation, Dept. Elect. Eng., Politecnico di Torino, Turin, Italy, 2002.

[22] R. Bojoi, F. Farina, M. Lazzari, F. Profumo, and A. Tenconi, "Analysis of the asymmetrical operation of dual three-phase induction machines," in *Proc. IEEE Int. Elect. Mach. Drives Conf.*, 2003, pp. 429–435.

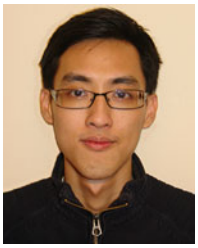

Hang Seng Che (M'14) received the B.Eng. degree in electrical engineering from the University of Malaya, Kuala Lumpur, Malaysia, in 2009, and the Ph.D. degree in electrical engineering under the auspices of a dual Ph.D. program between the University of Malaya and Liverpool John Moores University, Liverpool, U.K., in 2013.

Since 2013, he has been with UM Power Energy Dedicated Advanced Center, University of Malaya, where he is currently a Senior Lecturer. His research interests include multiphase machines and drives, fault-tolerant control, and power electronic converters for renewable energy applications.

Dr. Che has been an Associate Editor for *IET Electric Power Applications* since 2016. He received the 2009 Kuok Foundation Postgraduate Scholarship Award for his Ph.D. studies.

Ayman Samy Abdel-Khalik (SM'12) received the B.Sc. and M.Sc. degrees in electrical engineering from Alexandria University, Alexandria, Egypt, in 2001 and 2004, respectively, and the Ph.D. degree from Alexandria University and Strathclyde University, Glasgow, U.K., in 2009, under a dual channel program.

From 2009 to 2014, he was a Senior Research Scientist with Spiretronic LLC, Houston, TX, USA. He is currently an Associate Research Scientist at Texas A&M University at Qatar, Doha, Qatar. He is also an Associate Professor in the Electrical Engineering Department, Faculty of Engineering, Alexandria University. His current research interests include electrical machine design, electric machine simulation, electric drives, energy conversion, renewable energy, power quality, and HVDC.

Obrad Dordevic (S'11–M'13) received the Dipl.Ing. degree in electronic engineering from the University of Belgrade, Belgrade, Serbia, in 2008, and the Ph.D. degree in electrical engineering from Liverpool John Moores University, Liverpool, U.K., in 2013.

He is currently a Lecturer at Liverpool John Moores University. His main research interests include the areas of power electronics, electrostatic precipitators, and advanced variable-speed multiphase drive systems.

Emil Levi (S'89–M'92–SM'99–F'09) received the M.Sc. and Ph.D. degrees in electrical engineering from the University of Belgrade, Belgrade, Yugoslavia, in 1986 and 1990, respectively.

From 1982 to 1992, he was with the Department of Electrical Engineering, University of Novi Sad, Novi Sad, Serbia. In May 1992, he joined Liverpool John Moores University, Liverpool, U.K., where he has been a Professor of electric machines and drives since September 2000.

Prof. Levi was the Co-Editor-in-Chief of the IEEE TRANSACTIONS ON INDUSTRIAL ELECTRONICS during 2009–2013, and is currently the Editor-in-Chief of *IET Electric Power Applications* and the Editor of the IEEE TRANSACTIONS ON ENERGY CONVERSION. He received the Cyril Veinott Award of the IEEE Power and Energy Society for 2009 and the Best Paper Award of the IEEE TRANSACTIONS ON INDUSTRIAL ELECTRONICS for 2008. In 2014, he received the "Outstanding Achievement Award" from the European Power Electronics Association.